Observation of Solvent Penetration during Cold Denaturation of *E. coli* Phosphofructokinase-2

César A. Ramírez-Sarmiento,[†] Mauricio Baez,[‡] Christian A. M. Wilson,[†] Jorge Babul,[†] Elizabeth A. Komives,[§*] and Victoria Guixé[†*]

[†]Departamento de Biología, Facultad de Ciencias, Universidad de Chile, Santiago, Chile; [‡]Departamento de Bioquímica y Biología Molecular, Facultad de Ciencias Químicas y Farmacéuticas, Universidad de Chile, Santiago, Chile; and [§]Department of Chemistry and Biochemistry, University of California San Diego, La Jolla, California

ABSTRACT Phosphofructokinase-2 is a dimeric enzyme that undergoes cold denaturation following a highly cooperative $N_2 \Leftrightarrow 2I$ mechanism with dimer dissociation and formation of an expanded monomeric intermediate. Here, we use intrinsic fluorescence of a tryptophan located at the dimer interface to show that dimer dissociation occurs slowly, over several hours. We then use hydrogen-deuterium exchange mass spectrometry experiments, performed by taking time points over the cold denaturation process, to measure amide exchange throughout the protein during approach to the cold denatured state. As expected, a peptide corresponding to the dimer interface became more solvent exposed over time at 3°C; unexpectedly, amide exchange increased throughout the protein over time at 3°C. The rate of increase in amide exchange over time at 3°C was the same for each region and equaled the rate of dimer dissociation measured by tryptophan fluorescence, suggesting that dimer dissociation and formation of the cold denatured intermediate occur without appreciable buildup of folded monomer. The observation that throughout the protein amide exchange increases as phosphofructokinase-2 cold denatures provides experimental evidence for theoretical predictions that cold denaturation primarily occurs by solvent penetration into the hydrophobic core of proteins in a sequence-independent manner.

INTRODUCTION

Protein stability can be altered via perturbation of several properties that are required to ensure a properly folded state. Changes in pH, addition of chaotropic agents, high pressure, and increase in temperature have been successfully applied to drive proteins through their global unfolding transitions (1). Interestingly, it has been shown that the Gibbs free energy difference between the native and denatured state for a two-state system reaches zero at two different temperatures, thus suggesting that thermal unfolding transitions of proteins can be induced both on cooling and heating (2). As thermal stability of proteins is dominated by the concave free energy dependence with temperature, it has been predicted that proteins with large and positive ΔCp and small ΔH values would permit the observation of cold-induced unfolding/denaturation at temperatures above the freezing point of water (3,4).

Cold denaturation phenomena in proteins have been studied by several techniques, including spectroscopy (5), calorimetry (6), NMR (7), and molecular dynamics (8). However, with the exception of NMR experiments, these techniques only account for global properties and do not allow measurement of local changes during cold-induced denaturation. NMR is still limited by the size of the protein and requirement for specific labeling. Therefore, a better description of the cold denaturation process may be obtained by analysis of local changes in the structure of proteins using amide hydrogen-deuterium (H/D) exchange. H/D exchange followed by mass spectrometry (HXMS) is a powerful tool for studying protein-protein interactions (9), protein dynamics upon binding, and intrinsically disordered regions in proteins (10,11). The extent of exchange probes the solvent accessibility of amide protons, whereas the approach in which the exchange reaction is quenched, the protein is digested with pepsin, and the resulting peptides are analyzed by mass spectrometry, allows sampling of these changes over local regions of the protein.

Escherichia coli phosphofructokinase-2 (Pfk-2) is a homodimer of 66 kDa and one of the largest proteins that shows thermal unfolding transitions upon cooling and heating (12). Reversible thermal unfolding experiments under equilibrium conditions have shown that the cold-induced transition of Pfk-2 proceeds above the freezing point of water without requiring additional perturbations such as chaotropic agents (13,14), high pressure (15), extreme pH (16), or point mutations (17,18). Moreover, it has been shown that cold denaturation of Pfk-2 follows a two-state mechanism to a populated intermediate state ($N2 \Leftrightarrow 2I$) and it has been suggested that this process is highly cooperative, occurring concomitantly with dimer dissociation and leading to an expanded monomeric conformation that shows striking similarities to the guanidine HCl-induced monomeric intermediate (12).

In this work, we first used analytical ultracentrifugation to determine the amount of dimeric and monomeric species

Submitted December 19, 2012, and accepted for publication April 12, 2013.

*Correspondence: ekomives@ucsd.edu or vguixe@uchile.cl

Christian A. M. Wilson's present address is QB3 Institute, University of California at Berkeley, Berkeley, CA 94720.

Editor: Patricia Clark.

0006-3495/13/05/2254/10 $2.00

http://dx.doi.org/10.1016/j.bpj.2013.04.024

under equilibrium conditions spanning temperatures between 2 and 25°C, followed by intrinsic fluorescence measurements to study the kinetics of the unbiased cold denaturation of Pfk-2. Finally, we probed the amide exchange of the protein along the cold denaturation process with HXMS. We find that cold denaturation of Pfk-2 is a slow process that occurs without buildup of folded monomer. The amide exchange results reveal local increases in amide exchange that occur throughout Pfk-2 during cold challenge, leading to the monomeric intermediate state. We show that amide exchange increases throughout the protein as cold denaturation proceeds. Because the cold denaturation process is slow, the rate at which amide exchange increases at locations throughout the protein core could be ascertained by measuring HXMS in samples removed from the denaturation reaction at different times. Remarkably, the rate of increase in amide exchange was the same for all regions of the protein, and also matched the rate of monomer formation measured by tryptophan fluorescence. The results provide experimental validation of recently proposed theories of solvent penetration throughout the folded core of the protein as the mechanism of cold denaturation (19).

EXPERIMENTAL PROCEDURES

Purification and storage of Pfk-2

Pfk-2 was purified and stored as described by Babul (20). Before performing kinetic denaturation experiments, the storage buffer was changed to standard buffer (50 mM Tris pH 8.2, 5 mM $MgCl_2$, and 2 mM DTT) by centrifugation using a Micro Bio-Spin 6 column (BioRad Laboratories Inc., Hercules, CA). The enzyme was concentrated using a VivaSpin 3 concentrator (Sartorius Stedim Biotech S.A., Goettingen, Germany) when required. Protein concentration was determined by Bradford assay (21) using bovine serum albumin as standard and is expressed in terms of monomer concentration.

Sedimentation analysis by analytical ultracentrifugation at different temperatures

To ascertain the temperature at which Pfk-2 was completely monomeric, sedimentation velocity experiments were conducted at different temperatures. A Beckman Optima XL-I analytical ultracentrifuge (Beckman Coulter, Brea, CA) equipped with an An60Ti rotor was used for the experiments. Pfk-2 was exchanged from its storage buffer to 50 mM Tris pH 8.2, 5 mM $MgCl_2$, and 2 mM TCEP before the experiment. Pfk-2 samples (~38 μM) were incubated for 24 h at each desired temperature (from 2 to 25°C) to ensure equilibrium conditions and then placed in the analytical cells for centrifugation at a rotor speed of 42,000 rpm until complete sedimentation was achieved. The rotor, centrifuge, and analytical cells were equilibrated at the desired temperature before loading the samples. The moving boundary was monitored by absorbance at 280 nm. The resulting data were analyzed using different models. First, we used SEDFIT and the two-dimensional model of distribution of sedimentation coefficient and frictional ratio $c(S,ff_o)$ for analysis of the monomeric and dimeric species free from assumptions about the frictional ratio (22). This analysis was only performed at 4 and 25°C, where single species rather than monomer/dimer mixtures were expected. Distributions were obtained with equidistant fr-grid values between 0.8 and 2.2 in 0.1 steps, and linear S-grid values ranging from 0.5 to 6.5 in 0.1 steps. Data are presented in terms of $S_{20,w}$ and R_h, where $S_{20,w}$ corresponds to the sedimentation coefficient normalized to 20°C and water, and R_h is the Stokes radius. Two other models from SEDPHAT were then used: i), a simple global analysis of species to obtain the partial concentration of each monomer and dimer at each temperature (23), and ii), a self-association monomer-dimer model to compare the kinetic rates of dissociation estimated from our different measurements (24).

Rate of change of intrinsic tryptophan fluorescence over time in the cold

Kinetic denaturation of Pfk-2 was measured by intrinsic fluorescence, using its single tryptophan (W88) located on the interface between subunits as probe. Measurements were done in a Shimadzu PC-5031 spectrofluorometer (Shimadzu Europa GmbH, Duisburg, Germany). The change in intrinsic fluorescence was measured over time at 3°C. The protein was excited at a wavelength of 295 nm and the change was followed at 346 nm. The protein concentration used was 0.3 μM and the decay in signal was adjusted to an exponential decay to a minimum corresponding to the signal of the protein after 24 h at 3°C.

$$F = F_0 e^{-kt} + F_f \quad (1)$$

where F is the fluorescence intensity as a function of time t, F_0 is the fluorescence at $t = 0$ h, F_f is the fluorescence intensity recorded after 24 h at 3°C, and k is the rate of decay of the fluorescence signal.

Native state backbone amide exchange at 25°C

Pfk-2 backbone amide exchange was performed as previously described (10). The enzyme was incubated at room temperature for 2 h in standard buffer before starting the experiments. The exchange reaction was initiated when 80 μM of Pfk-2 was diluted 10-fold into D_2O. The protein was allowed to exchange at room temperature for 0–10 min. Exchange was quenched by diluting the sample 10-fold into 0.1% trifluoroacetic acid (TFA) in H_2O. Quenched protein was digested with pepsin as described and small aliquots of the digested sample were rapidly frozen in liquid N_2 and stored at −80°C.

Backbone amide exchange during cold denaturation

Pfk-2 was cold denatured by incubating the enzyme at 3°C. At several time points during the 12 h incubation, samples were removed and subjected to exchange in D_2O as described previously, and the exchange rate was measured between 0 and 40 min. The reaction was quenched into 0.1% TFA in H_2O and samples were digested and stored as described. To compare the denatured intermediate formed by cold denaturation with that formed at low guanidine concentrations, experiments were also performed on Pfk-2 diluted in 0.85 M guanidine HCl for 48 h, as in Baez and Babul (25). These experiments were performed at room temperature and exchange was monitored for 0–10 min, quenched, digested, and analyzed as described previously.

Digestion of Pfk-2 and identification of peptic peptides

After completion of the exchange reaction and quenching of amide exchange, Pfk-2 was digested with immobilized pepsin (Pierce Scientific, Rockford, IL) as previously described (10). Immobilized pepsin slurry (25 μL) was activated by washing twice with 0.1% TFA at pH 2.2. The protein was diluted in 0.1% TFA at pH 2.2 before incubation with immobilized pepsin for 5 min. Peptides were identified by MS/MS using a 4800 Plus

MALDI-TOF-TOF (AB SCIEX, Framingham, MA) and spectral analysis using MASCOT (Matrix Science, Boston, MA) and Protein Prospector.

Mass spectrometry

Matrix-assisted laser desorption/ionization time of flight (MALDI-TOF) mass spectra were acquired on a Voyager DE-STR instrument (Applied Biosystems, Carlsbad, CA) as previously described (26). The matrix used was 4.5 mg/mL α-Cyano-4-hydroxycinnamic acid (Sigma-Aldrich, St. Louis, MO) in a solution of 1:1:1 acetonitrile/ethanol/0.1% TFA. The pH of the matrix was adjusted to pH 2.2 using 2% TFA. The matrix solution and MALDI-TOF target plates were equilibrated at 4°C before the experiment as previously described (26).

MALDI-TOF mass spectra were analyzed as previously described (9,10), correcting for both side-chain contributions due to residual deuterium (4.5%) and back-exchange loss (50%). Plots were fit to a one-parameter exponential by using KaleidaGraph version 4.0 (Synergy Software, Reading, PA).

To calculate the kinetic denaturation rates (k), the maximum extent of exchange for each peptide as a function of time of exposure at cold temperature was fitted to an exponential rise to maximum:

$$E(t) = E_0 + N\left(1 - e^{-kt}\right) \quad (2)$$

where $E(t)$ is the maximum extent of exchange upon time, E_0 is the maximum extent of exchange at $t = 0$ h (i.e., extent of exchange for native state Pfk-2), N is the amplitude of the change in deuterons incorporated (i.e., the amount of backbone amides that begin to exchange due to changes in solvent accessibility), and t is the time of incubation at cold temperature.

Some samples were also analyzed on a Synapt G2 mass spectrometer (Waters, Milford, MA) following protocols described by Engen and co-workers (27) and these data were analyzed by PLGS and DynamX software packages.

RESULTS

Sedimentation analysis of Pfk-2 at different temperatures

To determine the equilibrium distribution of monomer and dimer species at different temperatures between 25 and 4°C, samples were equilibrated for 24 h and then analyzed by sedimentation velocity (Fig. 1). The protein is mainly a dimer at 25°C. Both monomers and dimers are present at temperatures between 8 and 15°C. At temperatures below 6°C almost all of the protein exists as a monomer. Furthermore, a Stokes radius larger than expected for a compact monomer is observed at 4°C (Fig. 1 *A*), in agreement with previous dynamic light scattering (DLS) experiments (12). This experiment established that cold-dependent dissociation to a monomer occurs (Fig. 1 *B*) and that to reach the endpoint of this transition, it is necessary to incubate the protein at a temperature of 4°C or lower.

Rate of Pfk-2 dissociation over time at 3°C

Typically, cold denaturation experiments are performed with the concomitant addition of chaotropic agents to facilitate the denaturation process. Because we knew that Pfk-2 denatures completely to the monomer at 3°C without the addition of chaotropic agents, we measured the rate of dissociation at 3°C over time taking advantage of the single tryptophan residue (W88) located on the dimer interface (Fig. 2). The rate of decay of the fluorescence signal over time of incubation at 3°C was 1.26×10^{-4} s^{-1}, which corresponds to a relatively slow conversion to monomer from dimer, on the order of hours. Another estimation of the dissociation rate was obtained from sedimentation velocity experiments using a monomer-dimer self-association model (24), which gave $k_{off} = 0.8 \times 10^{-4}$ s^{-1} $\pm$ 0.3×10^{-4} s^{-1}). The fact that conversion to the cold-denatured intermediate state is slow, but can be observed without the addition of chaotropic agents, prompted us to carry out amide exchange experiments over the cold denaturation process to investigate how the Pfk-2 molecules change as cold denaturation occurs.

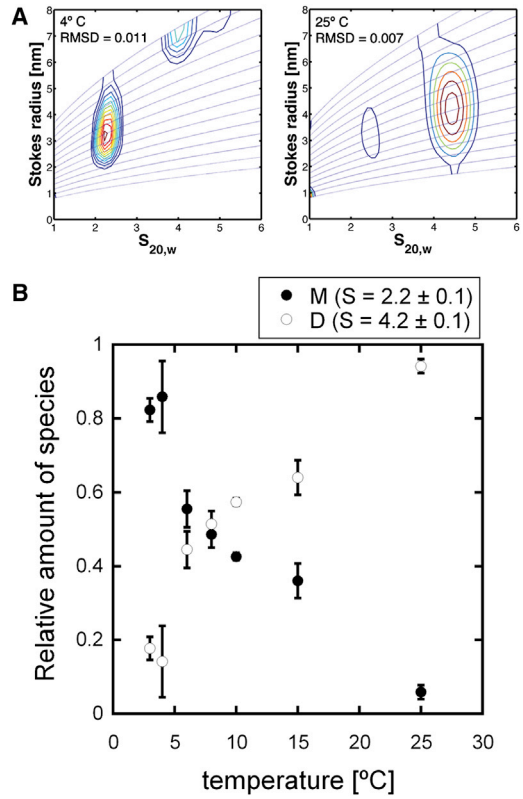

FIGURE 1 (*A*) Contour plots of the two-dimensional distribution in terms of $S_{20,w}$ and Stokes radius of Pfk-2 monomers and dimers at 4 and 25°C. Data were obtained by sedimentation velocity experiments and subsequent analysis using a continuous $c(S,ff_o)$ model, here represented as $c(S_{20,w},R_h)$. The magnitude of $c(S_{20,w},R_h)$is indicated by the color of the contours in equidistant intervals of c from blue (*low, outer boundary of each contour*) to red (*high, center of each contour*). The dotted lines indicate lines of constant f_r. The RMSD resulting from fitting the data is indicated. (*B*) Plot of the percent of monomer (*solid circles*) and dimer (*open circles*) at each temperature measured as calculated from the global analysis of species using SEDPHAT. The sedimentation coefficient values indicated were obtained from fitting the data and are similar between the different models used.

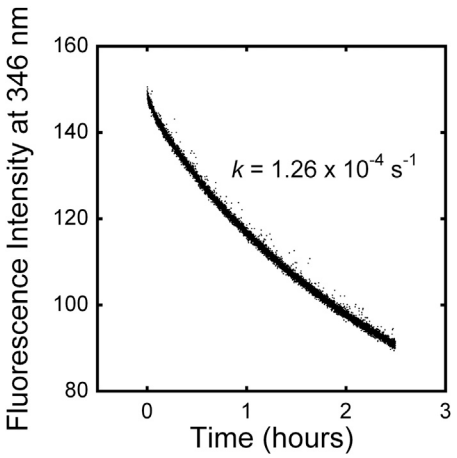

FIGURE 2 Intrinsic fluorescence measurement of Pfk-2 during cold denaturation at 3°C. The kinetic constant for dissociation (k) was calculated by fitting the data to an exponential decay curve.

Native state amide exchange of Pfk-2 at 25°C

To discover whether there were temperature-dependent differences in the amide exchange of Pfk-2 at 25 and 3°C, we performed HXMS experiments. As a control, Pfk-2 was allowed to exchange under native conditions for 10 min at 25°C. The samples were quenched by dilution into ice cold 0.1% TFA, digested for 5 min with immobilized pepsin, and analyzed on the MALDI-TOF mass spectrometer. Several peptides could be analyzed quantitatively, and these represented ~27% coverage of protein sequence (Table 1, Fig. S1 in the Supporting Material). These peptides are distributed throughout the protein structure, including a single peptide spanning residues 104–113 (MH+ 1124.592) that corresponds to one of the β-strands of the interface, thus working as a reporter of the interface between subunits. At 25°C, Pfk-2 had little solvent accessibility (Fig. S2). Experiments were not carried out to achieve complete exchange, but rather to measure the more rapidly exchanging amides. Most regions of Pfk-2, including the interfacial peptide that reports on association between monomers, exchanged 23% on average after 5 min in D_2O. Residues 1–7 of the protein (MH+ = 895.507) exchanged 43% (Fig. S2), suggesting that the N-terminus of Pfk-2 is more solvent accessible than the well-packed protein core.

Native state amide exchange of Pfk-2 at 3°C

As a control for the planned kinetic analysis of amide exchange during cold denaturation, we performed an experiment in which Pfk-2 was diluted into buffer preequilibrated at 3°C. This important control accounts for any temperature effects of the buffer on the amide exchange rates and also serves as a 0 time point for measuring the rate of change of the amide exchange over the very slow cold denaturation process (occurring over 12 h). According to Bai et al., the exchange is expected to be fourfold slower at 3°C compared to 25°C, so the HXMS time points were measured over 40 min instead of over 10 min (28).

To compare the HXMS of Pfk-2 at 25°C (Fig. S2) and immediately after dilution to 3°C (Fig. S3), we compared the total and backbone solvent accessible surface area (SASA) from Pfk-2 structure (PDB ID 3CQD) to the extent of amide exchange at 25°C (10 min time point) and to the extent of amide exchange of the sample immediately diluted to 3°C (40 min time point). In this manner, we wanted to confirm that the conformation of Pfk-2 at the beginning of the cold denaturation was the same as the conformation at room temperature.

The extent of amide exchange under both conditions was highly correlated with the backbone SASA for all covered regions of Pfk-2 as shown in Fig. 3 for the enzyme at 25°C or immediately diluted into buffer at 3°C (correlation coefficient 0.92 and 0.85, respectively). The results suggest that there is no significant change in Pfk-2 conformation after initial exposure to cold temperature consistent with the very slow rate of conversion to the cold-denatured intermediate observed by tryptophan fluorescence.

Cold-induced denaturation and dissociation of Pfk-2

Because the kinetics of cold-induced denaturation of Pfk-2 was so slow, we thought it would be possible to monitor the change in amide exchange at various times during the denaturation process. The experimental setup involved incubating Pfk-2 at 3°C for 12 h, and at intervals during this cold incubation, samples were removed and analyzed for the extent of amide exchange by diluting into deuterated buffer

TABLE 1 List of peptides quantified through MALDI-TOF mass spectrometry

Region of Pfk-2	Peptide mass (m/z)	No. amides	Relative exchange 4°C/25°C	Sequence
1–7	895.507	7	>	MVRIYTL
276–285	934.511	10	>	VRFGVAAGSA
286–294	973.543	9	>	ATLNQGTRL
275–285	1065.551	11	>	MVRFGVAAGSA
104–113	1124.592	9	>	YRFVMPGAAL
118–126	1161.626	9	>	FRQLEEQVL
154–164	1174.636	11	>	SAAQKQGIRCI
44–69	2445.300	25	>	VARAIAHLGGSATAIFPAGGATGEHL

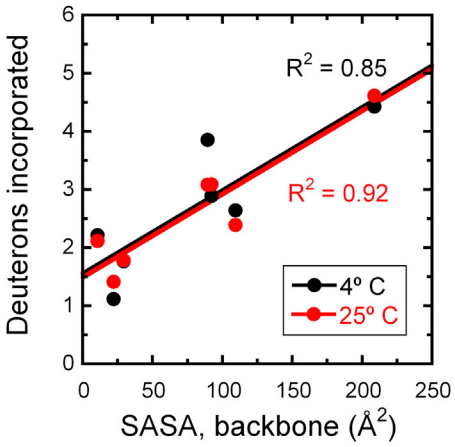

FIGURE 3 Correlation between backbone SASA calculated from Pfk-2 crystal structure (PDB ID 3CQD) and backbone amide exchange reactions at room temperature (*red*) and immediately after the Pfk-2 was exposed to cold temperature (*black*).

and monitoring deuterium incorporation into each region of the protein over 40 min as described previously. This experiment follows the change in amide exchange for each peptide representing different regions of the protein and the dimer interface over the entire time course of cold denaturation (Fig. 4).

As shown in Fig. 2, Pfk-2 denatures to a monomeric intermediate over hours of incubation at 3°C. Therefore, we expected (and observed) that the peptide corresponding to residues 104–113 (MH+ 1124.592), representing one of the β-strands that forms the dimer interface, would exchange more as the protein denatured to the monomeric state. To obtain these data, we plotted the maximum exchange (i.e., the extent of exchange at 40 min) observed for samples removed after 2, 4, 8, and 12 h of incubation of Pfk-2 at 3°C (Figs. S4–S7). The extent of deuteration for these samples represents the change in amide exchange of each region of Pfk-2 during the cold denaturation process. It was not surprising that the dimer interface becomes more solvent accessible as the protein becomes monomeric during the denaturation process, however, the results from the peptides corresponding to other regions of Pfk-2 were very much unexpected. Remarkably, all of the regions of Pfk-2 corresponding to peptides we could analyze by MALDI-TOF mass spectrometry showed increasing amide exchange when Pfk-2 was incubated at 3°C over several hours. The extent of exchange reached a plateau at <100% backbone amide exchange and longer times of deuteration were not explored (11,29). The plateauing amide exchange is consistent with a partially folded state in agreement with previous data showing that Pfk-2 reaches an intermediate state and not a completely unfolded state upon cold denaturation (12). Moreover, the extent of exchange of the cold-induced species was less than the exchange observed for the chemically induced intermediate at room temperature in 0.85 M guanidine HCl (Fig. 5). The increase in solvent accessibility over the cold denaturation at 3°C could be fitted to a single exponential rate

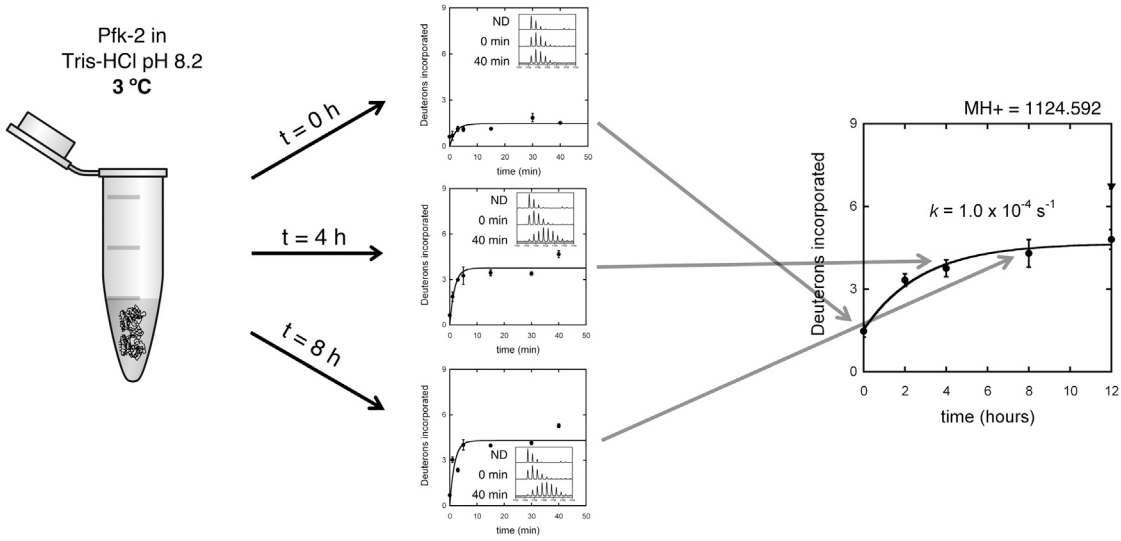

FIGURE 4 Schematic of the experimental approach to monitoring solvent penetration over time during cold denaturation. The protein was equilibrated to 3°C, and samples were removed at times 0, 2, 4, 8, and 12 h. The sampling was based on the slow rate of conversion to the cold-denatured intermediate measured by fluorescence (Fig. 2). After the sample was removed, it was diluted into deuterated buffer and allowed to exchange over 40 min during which time samples of this reaction were removed and the extent of exchange was measured for each time point. The plots of exchange over 40 min immediately after equilibration at 3°C (0 h) are shown in Fig. S3; the plots of exchange after equilibration at 3°C for 2 h are shown in Fig. S4; the plots of exchange after equilibration at 3°C for 4 h are shown in Fig. S5; the plots of exchange after equilibration at 3°C for 8 h are shown in Fig. S6; and the plots of exchange after equilibration at 3°C for 12 h are shown in Fig. S7. From these plots, the extent of deuteration (amount of deuteration at 40 min) was determined and plotted against the time at 3°C in hours. These are the data that are presented in Fig. 5.

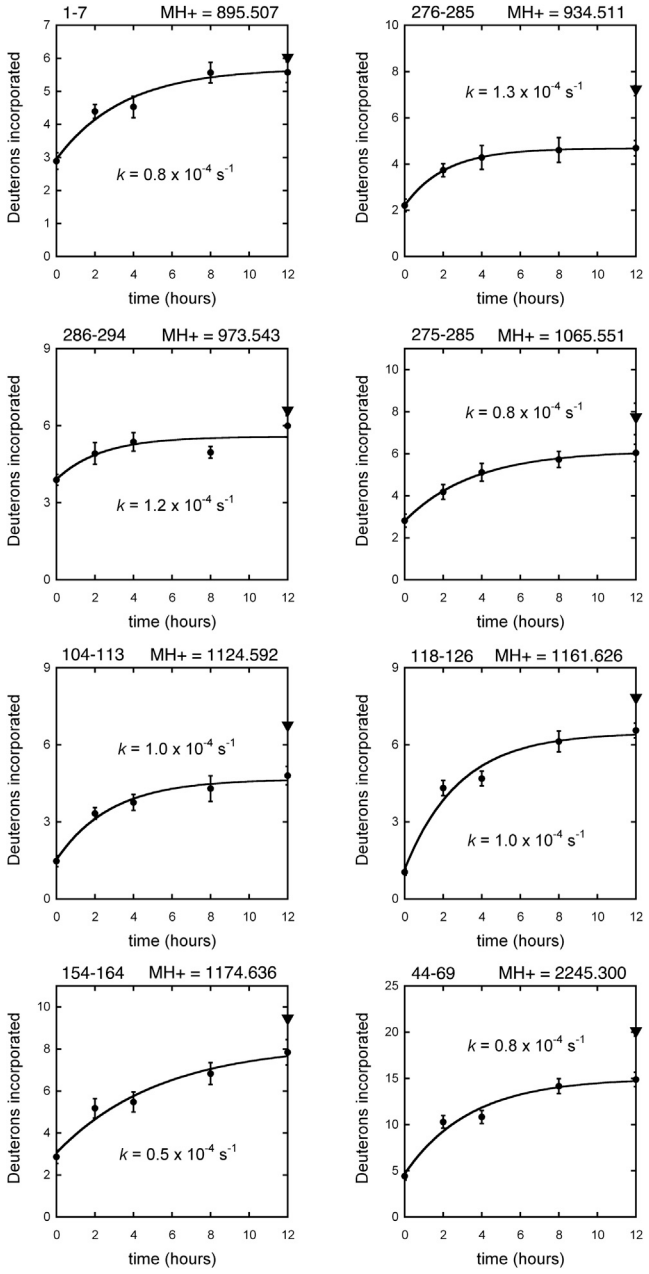

FIGURE 5 Cold denaturation of Pfk-2 followed by backbone amide exchange. Each plot represents the change in deuterons incorporated after 40 min for each peptide as a function of time during exposure to cold temperature. The *y* axis represents the number of exchangeable amides in the particular peptide. The kinetic constant (k) was calculated by fitting the data to an exponential curve. Triangles indicate the deuterons incorporated after 10 min of exchange for Pfk-2 incubated in 0.85 M guanidine HCl. The results suggest that the cold-induced monomeric intermediate is similar to the intermediate induced by guanidine HCl however it may be slightly more compact.

curve, and the rates for each different region of Pfk-2 were very similar for the different regions, $1.0 \times 10^{-4} \pm 0.25 \times 10^{-4}$ s^{-1} (Fig. 5). The peptide that covered the dimer interface also increased solvent accessibility at the same rate, indicating that dissociation and denaturation are concurrent processes during cold denaturation of the enzyme. The rate of increase in amide exchange during cold denaturation was very similar to the rate of cold denaturation estimated by measuring the decay of the fluorescence signal from the single tryptophan (W88) located on the interface between both subunits (Fig. 2) reinforcing the idea that the dimer dissociation and increased amide exchange throughout Pfk-2, which both occur upon incubation of Pfk-2 for several hours at 3°C, likely represent the same denaturation process. In keeping with the cooperative nature of the denaturation process, some of the mass envelopes (cf. Figs. S5 and S6) eventually appeared bimodal indicating an EX1-type of exchange process that would be expected if the dimer (less exchanging) converted to the expanded monomer (more exchanging) without formation of other intermediates.

The peptides that could be analyzed from the MALDI-TOF HXMS were distributed throughout the protein, but only 27% of the protein sequence was covered. The peptides we analyzed all increased in the extent of deuteration over time in the cold suggesting that the protein globally expanded (Fig. S8). To strengthen this conclusion, additional HXMS data were collected on a Synapt G2 HDX instrument. Due to limitations of instrument time, only one time point of cold denaturation could be studied. The protein was incubated at either 25 or 4°C for 6 h, and amide exchange was measured for time points of 0, 2, 5, and 10 min after incubation. The peptides that could be analyzed quantitatively covered 100% of the protein sequence (Table 2). All regions of Pfk-2 showed increased deuteration after incubation in the cold, recapitulating the MALDI-TOF data, except for two peptides that covered the active site catalytic residues, which showed identical exchange at both temperatures. Thus, these additional data suggest that the entire protein except the catalytic center expands during cold denaturation.

DISCUSSION

The mechanism of cold denaturation remains controversial. Some reports suggest the process is noncooperative (30), whereas other reports suggest that at least for Yfh1 and the C-terminal domain of L9, it is highly cooperative (7,31). Questions also remain as to whether the cold denatured state is compact, and whether it contains only native structure or also nonnative structure (32,33). These discrepancies arise from several factors: i), commonly, proteins cold denature at temperatures below the freezing point of water, a problem that can be circumvented by an additional perturbation but with the cost of moving away from physiological conditions; ii), the unfolding rate strongly depends on temperature, being several times slower at temperatures close to 0°C and thus making the cold-denatured state kinetically inaccessible (34). Recent results from DSC have

TABLE 2 List of peptides identified through MS^e mass spectrometry and relative exchange at 4 and 25°C

Region of Pfk-2	Peptide mass (m/z)	No. amides	Relative exchange 4°C/25°C	Ratio avg. exchange 25°C/4°C	Sequence
1–13	1477.844	9	>	0.87	MVRIYTLAPSL
2–13	1346.804	8	>	0.88	VRIYTLAPSL
14–69	5514.822	50	>	0.89	DSATITPQIYPEGKLRCTAPVFEPGGGGINVARAIAHL GGSATAIFPAGGATGEHL
33–69	3469.797	34	>	0.89	PVFEPGGGGINVARAIAHLGGSATAIFPAGGATGEHL
44–69	2445.299	24	>	0.78	VARAIAHLGGSATAIFPAGGATGEHL
44–72	2744.484	27	>	0.87	VARAIAHLGGSATAIFPAGGATGEHLVSL
73–84	1256.636	10	>	0.88	LADENVPVATVE
73–103	3442.698	29	>	0.89	LADENVPVATVEAKDWTRQNLHVHVEASGEQ
73–113	4548.272	38	>	0.88	LADENVPVATVEAKDWTRQNLHVHVEASGEQYRFVMPGAAL
104–113	1124.592	8	>	0.92	YRFVMPGAAL
104–117	1611.747	12	>	0.95	YRFVMPGAALNEDE
118–126	1161.626	8	>	0.59	FRQLEEQVL
119–126	1014.557	7	>	0.57	RQLEEQVL
127–134	831.446	6	>	0.9	EISGAIL
134–163	3147.828	28		0.94	LVISGSLPPGVKLEKLTQLISAAQKQGIRC
135–163	3034.744	27		0.94	VISGSLPPGVKLEKLTQLISAAQKQGIRC
164–175	1119.552	11	=	1.0	IVDSSGEALSAA
164–176	1232.636	12	=	1.05	IVDSSGEALSAAL
177–183	729.414	6	=	1.0	AIGNIEL
183–238	5968.203	52	>	0.95	LVKPNQKELSALVNRELTQPDDVRKAAQEIVNSGKAKRV VVSLGPQGALGVDSENC
239–260	2153.127	18	=	1.06	IQVVPPPVKSQSTVGAGDSMVG
239–263	2456.252	21	=	1.0	IQVVPPPVKSQSTVGAGDSMVGAMT
239–264	2569.337	22	=	0.96	IQVVPPPVKSQSTVGAGDSMVGAMTL

shown that the unfolding rates are, in fact, highly important to ensure an adequate definition of the energetic and structural features of the unfolding process. The slow unfolding rate at low temperatures due to a high folding/unfolding free energy barrier can lead to kinetic trapping in the initial distribution of states and therefore to misleading interpretations about the cooperativity of the cold denaturation process (34). Pfk-2 forms a cold-denatured intermediate that is monomeric and somewhat expanded at temperatures below 4°C. Because no nonphysiological perturbants are required, and because the denaturation process occurs over several hours (Figs. 2 and 5), Pfk-2 provides an excellent model system in which to study the cold denaturation process.

Backbone amide exchange and mass spectrometry to probe cold-induced protein denaturation

Backbone amide exchange measured by mass spectrometry (35) has been used to describe protein dynamics (26,36), protein-protein interactions (9,37), and intrinsically disordered regions (11,29). Here, we apply this technique to discover how amide exchange changes over the course of the slow cold denaturation of Pfk-2 that occurs without requiring additional perturbation (12). Although HXMS is a mid-resolution technique, it is not limited by the molecular weight of a particular protein and, in principle, it can be applied to study proteins with biased cold-induced denaturation or proteins that dissociate upon exposure to cold temperatures (38,39). Therefore, HXMS constitutes a powerful technique to describe changes in protein association and amide exchange upon denaturation. The combination of global probes (such as intrinsic fluorescence) with HXMS to describe local structure changes constitutes a powerful combined approach to analyze changes in protein association and amide exchange upon denaturation.

Rate of monomer formation during cold-induced protein denaturation

In previous work, the global probes of intrinsic tryptophan fluorescence and circular dichroism spectroscopy revealed the formation of an intermediate with residual secondary structure during kinetic unfolding of Pfk-2 in guanidine HCl (40). Incubation of Pfk-2 at 3°C resulted in the formation of a cold denatured species, which according to intrinsic tryptophan fluorescence, DLS, and circular dichroism resembled the guanidine HCl-induced unfolding intermediate (12). DLS revealed that the cold-denatured species was monomeric. Here, we confirmed by sedimentation velocity experiments that equilibration of Pfk-2 at 3°C results in complete formation of a monomeric species. The rate of formation of this cold-induced monomeric species of Pfk-2 as indicated by the global probe of intrinsic tryptophan fluorescence change, was slow; $k = 1.26 \times 10^{-4} \pm 0.04 \times 10^{-4}$ s^{-1} (Fig. 2). Another estimation of the dissociation rate was obtained from sedimentation velocity experiments using a

monomer-dimer self-association model, which was similar to the rate calculated by intrinsic fluorescence (k_{off} = 0.8×10^{-4} s^{-1} $\pm$ 0.3×10^{-4} s^{-1}) (24). We were able to monitor the change in amide exchange over time of incubation of Pfk-2 at 3°C for a peptide representing the dimer interface, and the rate of increasing amide exchange was $1.0 \times 10^{-4} \pm 0.26 \times 10^{-4}$ s^{-1}. Given that this peptide was at the dimer interface, we can conclude that the increased exchange is reporting on the monomer formation. The fact that the rates are within error suggests that the tryptophan at the interface and the change in amide exchange are monitoring the same phenomenon; monomer formation.

Observation of solvent penetration during cold denaturation

Because the cold denaturation of Pfk-2 occurs over hours of incubation at 3°C, we were able to probe changes in amide exchange throughout the protein during the denaturation process. As shown in Figs. 5 and 6, all of the peptides from regions throughout Pfk-2 showed an increase in the extent of backbone amide exchange as the protein is undergoing the slow process of cold denaturation. Thus, as Pfk-2 cold denatures, it adopts a monomeric, globally expanded structure. The C-terminal domain of L9 protein also adopts an expanded structure upon cold denaturation, as indicated by pulse-field gradient NMR diffusion experiments (32). As pointed out by these authors, this type of protein expansion is most likely due to the weakening of hydrophobic interactions upon cold denaturation (32). Consistent with the idea that the expanded cold denatured state becomes more solvent penetrated, we observed more and more amide exchange throughout the folded protein core over the course of Pfk-2 cold denaturation. The fact that all regions of the protein showed similar rates of increasing amide exchange is consistent with a model in which monomer formation and expansion are concurrent. No buildup of a folded monomeric species was detected. In addition, the fact that amide exchange increases throughout the protein suggests that the increased amide exchange is due to solvent penetration occurring as the protein cold denatures.

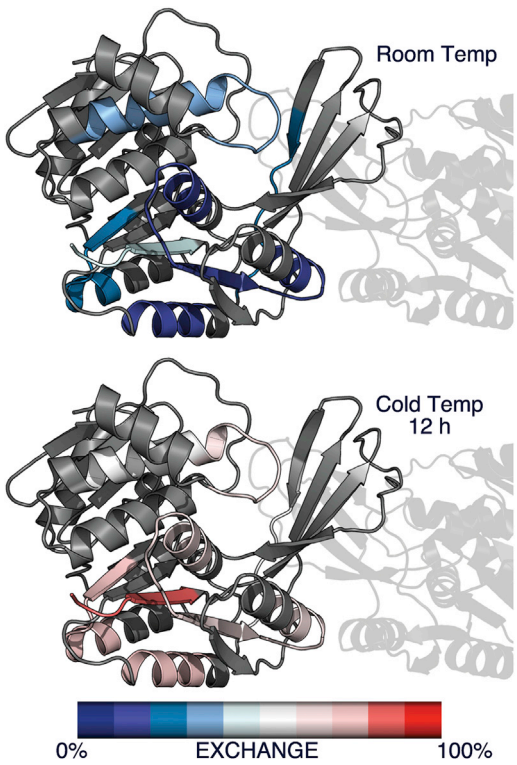

FIGURE 6 Change in solvent accessibility in the Pfk-2 structure upon cold denaturation. Peptides are colored according to their maximum exchange at room temperature (*top*) and after 12 h at cold temperature (*bottom*).

The HXMS experiments allowed us to monitor probes throughout the Pfk-2 structure over time. Remarkably, for all of the different regions of the protein covered in the HXMS experiments, the rate of increased amide exchange over time in the cold was similar, with an average rate of increase being $1.0 \times 10^{-4} \pm 0.25 \times 10^{-4}$ s^{-1}. These results strongly suggest that cold denaturation of this enzyme is accompanied by solvent penetration that occurs globally throughout the structure. The only exception to this assertion is the active site, which appears to remain compact according to additional HXMS data (Table 2).

Theoretical studies have also suggested that cold denaturation involves destabilization of hydrophobic contacts within the protein core in favor of solvent-separated configurations (41,42). This process is similar to that observed for pressure-induced unfolding (43). The theoretical studies reveal that at physiological temperatures, water molecules close to the protein have at least one nonsaturated H-bond, which is pointing toward the protein and they form a thin solvation shell. As the temperature decreases, the energy of the water H-bonds increases and cages of water molecules are formed, thus increasing the solvation shell. Coupled with the destabilization of hydrophobic interactions within the protein, hydration of the protein core is predicted to occur in a sequence-independent manner. Recent experimental studies on cold denaturation of proteins using water-^{17}O magnetic relaxation dispersion to characterize the single-molecule water dynamics in the hydration layer, provided information about the number of water molecules that interact directly with the protein and about their rotational correlation times. For a destabilized mutant of apomyoglobin and for α-lactoglobulin in 4 M urea, these authors concluded that the protein molecules remain "relatively compact and are better described as solvent-penetrated than as unfolded" (44).

CONCLUSION

Using HXMS, we have now been able to probe the local solvent accessibility of protein backbone NH groups and for

the first time, to our knowledge, obtain a view from the perspective of the protein, of solvent penetration during cold denaturation in the absence of other perturbants. Our results show a similar increase in solvent accessibility of the amides across the entire protein to a state that is apparently solvent penetrated, but still retains some degree of compaction. The proposed theoretical mechanism does not involve specific amino acid contacts, but rather appears to be a phenomenon of weakening of hydrophobic contacts and mostly a rearrangement of the water structure (45). One prediction of the theory is therefore that cold denaturation would affect the entire cooperatively folded core of the protein equally. The fact that local regions of Pfk-2 all increase solvent accessibility at equal rates during the cold denaturation process provides strong support for this theoretical prediction.

SUPPORTING MATERIAL

Eight figures, supporting legends, and references (46-47) are available at http://www.biophysj.org/biophysj/supplemental/S0006-3495(13)00457-8.

This work was partially supported by Fondo Nacional de Desarrollo Científico y Tecnológico (Fondecyt) grants 1110137 and 1090336. César A. Ramírez-Sarmiento was supported by a Comisión Nacional de Investigación Científica y Tecnológica (Conicyt) graduate fellowship, a joint Mejoramiento de la Calidad y Equidad de la Educación (MECESUP) and Sciences, Technology and Innovation Program for the Americas (STIPAs) fellowship UCH0717 and a MECESUP fellowship UCH0713. We gratefully acknowledge Dr. Jon Fitchett from Lilly Biotechnology Center of San Diego for providing access to the Synapt G2 mass spectrometer.

REFERENCES

1. Matthews, C. R. 1993. Pathways of protein folding. *Annu. Rev. Biochem.* 62:653–683.
2. Privalov, P. L. 1990. Cold denaturation of proteins. *Crit. Rev. Biochem. Mol. Biol.* 25:281–305.
3. Privalov, P. L., Griko YuV, …, V. P. Kutyshenko. 1986. Cold denaturation of myoglobin. *J. Mol. Biol.* 190:487–498.
4. Privalov, P. L., and S. J. Gill. 1988. Stability of protein structure and hydrophobic interaction. *Adv. Protein Chem.* 39:191–234.
5. Damaschun, G., H. Damaschun, …, D. Zirwer. 1993. Cold denaturation-induced conformational changes in phosphoglycerate kinase from yeast. *Biochemistry.* 32:7739–7746.
6. Richardson, 3rd, J. M., S. D. Lemaire, …, G. I. Makhatadze. 2000. Difference in the mechanisms of the cold and heat induced unfolding of thioredoxin h from *Chlamydomonas reinhardtii*: spectroscopic and calorimetric studies. *Biochemistry.* 39:11154–11162.
7. Adrover, M., V. Esposito, …, P. A. Temussi. 2010. Understanding cold denaturation: the case study of Yfh1. *J. Am. Chem. Soc.* 132:16240–16246.
8. Lopez, C. F., R. K. Darst, and P. J. Rossky. 2008. Mechanistic elements of protein cold denaturation. *J. Phys. Chem. B.* 112:5961–5967.
9. Mandell, J. G., A. M. Falick, and E. A. Komives. 1998. Identification of protein-protein interfaces by decreased amide proton solvent accessibility. *Proc. Natl. Acad. Sci. USA.* 95:14705–14710.
10. Hughes, C. A., J. G. Mandell, …, E. A. Komives. 2001. Phosphorylation causes subtle changes in solvent accessibility at the interdomain interface of methylesterase CheB. *J. Mol. Biol.* 307:967–976.
11. Truhlar, S. M., J. W. Torpey, and E. A. Komives. 2006. Regions of IkappaBalpha that are critical for its inhibition of NF-kappaB.DNA interaction fold upon binding to NF-kappaB. *Proc. Natl. Acad. Sci. USA.* 103:18951–18956.
12. Baez, M., C. A. M. Wilson, …, J. Babul. 2012. Expanded monomeric intermediate upon cold and heat unfolding of phosphofructokinase-2 from Escherichia coli. *Biophys. J.* 103:2187–2194.
13. Griko YuV, and V. P. Kutyshenko. 1994. Differences in the processes of beta-lactoglobulin cold and heat denaturations. *Biophys. J.* 67:356–363.
14. Mizuguchi, M., D. Hashimoto, …, K. Nitta. 2000. Cold denaturation of alpha-lactalbumin. *Proteins.* 38:407–413.
15. Kunugi, S., and N. Tanaka. 2002. Cold denaturation of proteins under high pressure. *Biochim. Biophys. Acta.* 1595:329–344.
16. Azuaga, A. I., M. L. Galisteo, …, P. L. Mateo. 1992. Heat and cold denaturation of beta-lactoglobulin B. *FEBS Lett.* 309:258–260.
17. Chen, B. L., W. A. Baase, and J. A. Schellman. 1989. Low-temperature unfolding of a mutant of phage T4 lysozyme. 2. Kinetic investigations. *Biochemistry.* 28:691–699.
18. Chen, B. L., and J. A. Schellman. 1989. Low-temperature unfolding of a mutant of phage T4 lysozyme. 1. Equilibrium studies. *Biochemistry.* 28:685–691.
19. Dias, C. L., T. Ala-Nissila, …, M. Grant. 2008. Microscopic mechanism for cold denaturation. *Phys. Rev. Lett.* 100:118101.
20. Babul, J. 1978. Phosphofructokinases from *Escherichia coli*. Purification and characterization of the nonallosteric isozyme. *J. Biol. Chem.* 253:4350–4355.
21. Bradford, M. M. 1976. A rapid and sensitive method for the quantitation of microgram quantities of protein utilizing the principle of protein-dye binding. *Anal. Biochem.* 72:248–254.
22. Brown, P. H., and P. Schuck. 2006. Macromolecular size-and-shape distributions by sedimentation velocity analytical ultracentrifugation. *Biophys. J.* 90:4651–4661.
23. Houtman, J. C., P. H. Brown, …, P. Schuck. 2007. Studying multisite binary and ternary protein interactions by global analysis of isothermal titration calorimetry data in SEDPHAT: application to adaptor protein complexes in cell signaling. *Protein Sci.* 16:30–42.
24. Schuck, P. 2003. On the analysis of protein self-association by sedimentation velocity analytical ultracentrifugation. *Anal. Biochem.* 320:104–124.
25. Baez, M., and J. Babul. 2009. Reversible unfolding of dimeric phosphofructokinase-2 from *Escherichia coli* reveals a dominant role of inter-subunit contacts for stability. *FEBS Lett.* 583:2054–2060.
26. Mandell, J. G., A. M. Falick, and E. A. Komives. 1998. Measurement of amide hydrogen exchange by MALDI-TOF mass spectrometry. *Anal. Chem.* 70:3987–3995.
27. Wales, T. E., K. E. Fadgen, …, J. R. Engen. 2008. High-speed and high-resolution UPLC separation at zero degrees Celsius. *Anal. Chem.* 80:6815–6820.
28. Bai, Y., J. S. Milne, …, S. W. Englander. 1993. Primary structure effects on peptide group hydrogen exchange. *Proteins.* 17:75–86.
29. Croy, C. H., S. Bergqvist, …, E. A. Komives. 2004. Biophysical characterization of the free IkappaBalpha ankyrin repeat domain in solution. *Protein Sci.* 13:1767–1777.
30. Pometun, M. S., R. W. Peterson, …, A. J. Wand. 2006. Cold denaturation of encapsulated ubiquitin. *J. Am. Chem. Soc.* 128:10652–10653.
31. Luan, B., B. Shan, …, D. P. Raleigh. 2013. Cooperative cold denaturation: the case of the C-terminal domain of the ribosomal protein L9. *Biochemistry.* 52:2402–2409.
32. Li, Y., B. Shan, and D. P. Raleigh. 2007. The cold denatured state is compact but expands at low temperatures: hydrodynamic properties of the cold denatured state of the C-terminal domain of L9. *J. Mol. Biol.* 368:256–262.
33. Shan, B. B., S. S. McClendon, …, D. P. Raleigh. 2010. The cold denatured state of the C-terminal domain of protein L9 is compact and

contains both native and non-native structure. *J. Am. Chem. Soc.* 132:4669–4677.

34. Romero-Romero, M. L., A. Inglés-Prieto, …, J. M. Sanchez-Ruiz. 2011. Highly anomalous energetics of protein cold denaturation linked to folding-unfolding kinetics. *PLoS ONE.* 6:e23050.

35. Zhang, Z., and D. L. Smith. 1993. Determination of amide hydrogen exchange by mass spectrometry: a new tool for protein structure elucidation. *Protein Sci.* 2:522–531.

36. Engen, J. R., T. E. Smithgall, …, D. L. Smith. 1997. Identification and localization of slow, natural, cooperative unfolding in the hematopoietic cell kinase SH3 domain by amide hydrogen exchange and mass spectrometry. *Biochemistry.* 36:14384–14391.

37. Engen, J. R., W. H. Gmeiner, …, D. L. Smith. 1999. Hydrogen exchange shows peptide binding stabilizes motions in Hck SH2. *Biochemistry.* 38:8926–8935.

38. Weber, G. 1993. Thermodynamics of the association and the pressure dissociation of oligomeric proteins. *J. Phys. Chem.* 97:7108–7115.

39. Foguel, D., and J. L. Silva. 1994. Cold denaturation of a repressor-operator complex: the role of entropy in protein-DNA recognition. *Proc. Natl. Acad. Sci. USA.* 91:8244–8247.

40. Baez, M., C. A. Wilson, and J. Babul. 2011. Folding kinetic pathway of phosphofructokinase-2 from *Escherichia coli*: a homodimeric enzyme with a complex domain organization. *FEBS Lett.* 585:2158–2164.

41. Oshima, H., T. Yoshidome, …, M. Kinoshita. 2009. A theoretical analysis on characteristics of protein structures induced by cold denaturation. *J. Chem. Phys.* 131:205102.

42. Das, P., and S. Matysiak. 2012. Direct characterization of hydrophobic hydration during cold and pressure denaturation. *J. Phys. Chem. B.* 116:5342–5348.

43. Panick, G., R. Malessa, …, C. A. Royer. 1998. Structural characterization of the pressure-denatured state and unfolding/refolding kinetics of staphylococcal nuclease by synchrotron small-angle X-ray scattering and Fourier-transform infrared spectroscopy. *J. Mol. Biol.* 275:389–402.

44. Davidovic, M., C. Mattea, …, B. Halle. 2009. Protein cold denaturation as seen from the solvent. *J. Am. Chem. Soc.* 131:1025–1036.

45. Levy, Y., and J. N. Onuchic. 2006. Water mediation in protein folding and molecular recognition. *Annu. Rev. Biophys. Biomol. Struct.* 35:389–415.

46. Parducci, R. E., R. Cabrera, …, V. Guixé. 2006. Evidence for a catalytic Mg2+ ion and effect of phosphate on the activity of *Escherichia coli* phosphofructokinase-2: regulatory properties of a ribokinase family member. *Biochemistry.* 45:9291–9299.

47. Bork, P., C. Sander, and A. Valencia. 1993. Convergent evolution of similar enzymatic function on different protein folds: the hexokinase, ribokinase, and galactokinase families of sugar kinases. *Protein Sci.* 2:31–40.